Reflective tomography: images from range-resolved laser radar measurements

Jeffrey K. Parker, E. B. Craig, D. I. Klick, F. K. Knight, S. R. Kulkarni, R. M. Marino, J. R. Senning, and B. K. Tussey

J. R. Senning is with University of Virginia, Charlottesville, Virginia 22901; E. B. Craig is with Ford Aerospace & Communications Corporation, Horsham, Pennsylvania 19044; and the other authors are with Massachusetts Institute of Technology, Lincoln Laboratory, Lexington, Massachusetts 02173-0073.

Received 20 January 1988.
0003-6935/88/132642-02$02.00/0.

The reconstruction of a 2-D image from a set of 1-D microwave reflective measurements has been studied by others in the radar community (see references contained in Ref. 1). Das and Boerner[2] have shown that the reconstruction of a 2-D radar image from 1-D reflective measurements is identical to the problem of determining a 2-D image from a set of 1-D transmission projections. This latter problem has been extensively studied in many fields ranging from medical imaging to radio astronomy. In this paper, we apply a well-known tomographic reconstruction technique to a series of 1-D range-resolved laser radar measurements to form a 2-D image of a cone. These new results extend methods of radar imaging used at microwave wavelengths into the optical regime.

Laser radar systems can provide measurements of 1-D range-resolved or 2-D range-Doppler-resolved target reflective signatures.[3,4] In the latter case, a 2-D image can be immediately formed. In some circumstances, however (e.g., slowly rotating objects), range-Doppler imaging with laser radar systems may be difficult.[5] In these cases, independent range-resolved measurements may still be possible yielding 1-D information about the object under study. In range-resolved radar imagery, the target is probed along a line that extends to, but not through, the target. The sensor obtains information only from those surfaces of the target illuminated by the radar. Such measurements can be viewed as a projection of the illuminated target surface resolved in the range dimension in discrete range steps. As such, the projection surfaces are those along which the range between the transmitter, target surface, and receiver are constant. Extending the work of Das and Boerner,[2] classical tomographic techniques can be applied to the problem of laser imagery, and a 2-D image of the object under study can be formed from 1-D projections measured in angular increments around the object.

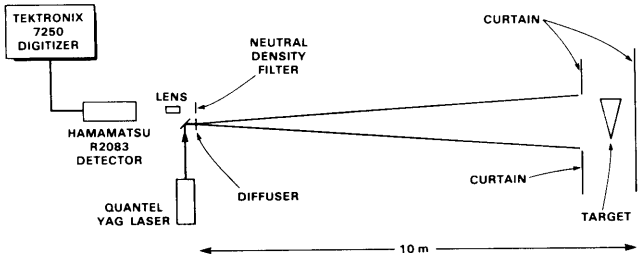

Fig. 1. Experimental apparatus used to measure range-resolved projections of a cone. The target was rotated about an axis slightly forward of the cone's geometric center and perpendicular to its body axis and the sensor line of sight, simulating a tumbling motion.

The experimental setup used to measure the range-resolved data is shown in Fig. 1. A cone-shaped test target (170-cm axial height × 53-cm base diameter) at a fixed aspect angle was illuminated by a 100 ps 532 nm pulse from a frequency-doubled Quantel mode-locked Nd:YAG laser. The return energy was distributed in time proportional to the range extent of the cone. The nearly monostatic return waveform was detected using a Hamamatsu R2083 photomultiplier and recorded every 100 ps with a Tektronix 7250 transient digitizer for a total time of 50 ns. Fifteen range-resolved measurements were recorded at each target aspect angle before transferring the data to a DEC μ-VAX computer. The cone aspect angle was then incremented and the process repeated. The target was rotated about an axis slightly forward of the cone's geometric center and perpendicular to its body axis and the sensor line of sight. The cone was symmetric about the axis of rotation and measured in 5° steps from 0° (tip forward) to 180° (base forward).

To prevent detector saturation, the return energy was attenuated using a different neutral density filter at each aspect angle. For calibration purposes, the digitizer time window was set to record the return energy from felt curtains both in front of and behind the target. The cross section of each curtain was constant during the experiment and was used to correct for the pulse-to-pulse laser amplitude fluctuations by normalizing all the data to the return from the curtains. The averaged, normalized, and scaled range-time-intensity return at each of the thirty-six different projection angles is shown in Fig. 2. Notice that the return from the target is distributed in time and is seen in range bins of 150–300. The return from the first curtain is contained in range bins of 0–100, and the return from the second curtain is contained in range bins of 300–400. The ultimate range resolution of the system was limited by the photomultiplier. The full width at half-maximum for the detector response was measured at 840 ps, yielding a range resolution of 12.6 cm. The laser wavefront curvature was negligible within a range cell so that the target is entirely contained within the beamwidth of an approximately plane-parallel wavefront. For the data presented, no attempt has been made to deconvolve the detector temporal response from the measured results.

The tomographic method of filtered backprojection[6,7] has

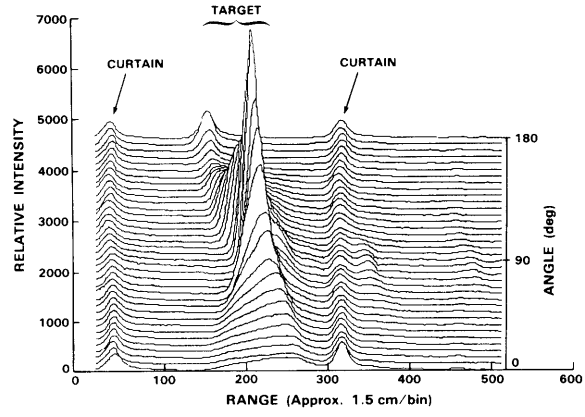

Fig. 2. Averaged, normalized, and scaled range-resolved reflected intensity data of a cone-shaped target as a function of range and projection angle. The target is symmetric about the body axis and was measured in 5° steps from 0 (tip forward) to 180° (base forward). The thirty-six range-resolved projection traces are separated for clarity.

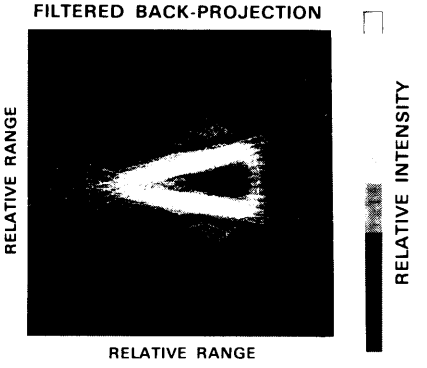

Fig. 3. Reconstructed image from measured range-resolved data of a cone-shaped target using the method of filtered backprojection.

been applied to the range-resolved measurements. This is a standard method of tomography, and only a brief description is provided. The simplest algorithm for image reconstruction is to estimate the value of the image $g(x,y)$ by spreading (backprojecting) the values of the projections $p(x\cos\phi_i + y\sin\phi_i,\phi_i)$ along the direction of projection and summing over all projection angles ϕ_i. This elementary method often produces streak artifacts in a starlike pattern resulting in a low-quality image estimate. To provide a better reconstruction, the projection profiles can be suitably modified before being backprojected by a filtering operation in which the magnitudes of the spatial frequency components of each projection are increased in proportion to their spatial frequency. The reconstructed image, $g_{FB}(x,y)$, using filtered backprojection is then given by

$$g_{FB}(x,y) = \sum_{i=1}^{m} q(x\cos\phi_i + y\sin\phi_i,\phi_i)\Delta\phi, \quad (1)$$

where the modified projections $q(r,\phi)$ are given by $q(r,\phi) = \mathcal{F}_1^{-1}\{|k|\mathcal{F}_1[p(r,\phi)]\}$ with $\mathcal{F}_1$ and $\mathcal{F}_1^{-1}$ denoting the Fourier and inverse Fourier transform operators and where ϕ_i is the angle of the ith projection, $\Delta\phi$ is the angular separation between projections, and m is the number of projections. Equation (1) is applied to the measured range-resolved projections given the initial angle of and the angular separation between projections.

The reconstructed image of the cone from the range-resolved measurements is shown in Fig. 3. The tip appears rounded due to the coarse range and angular resolution. The physical support for the cone was located at the base and was masked with a black felt covering causing the reconstructions of the base to appear dim. As is apparent, fair detail is realized using the method of filtered backprojection. From the projection data shown in Fig. 2 and knowledge of the range resolution of the radar, the target can be sized. The data indicate that the maximum and minimum range extents of the target are, respectively, 171 ± 12.6 and 48 ± 12.6 cm. This agrees well with the geometric maximum and minimum projections of 170 and 53 cm, respectively.

Summarizing: laser radar 1-D range-resolved measurements of a cone-shaped test target have been made, and high-resolution 2-D images have been formed using the tomographic method of filtered backprojection. Our work indicates that these data can be processed with other standard tomographic algorithms with similar results. To the authors' knowledge, these data are the first laser radar range-resolved measurements to be processed using tomographic reconstruction algorithms and present an extension into the optical regime of similar work done by others[2,8] at microwave wavelengths. This work indicates promise for future uses of laser radars. The issues of resolution, number of views, noise, more complicated target motions, and system applications will be addressed in future work.

This experiment could not have been done without the effort of many people. Special thanks to K. I. Schultz, A. L. Kachelmyer, R. E. Kowlden, and D. R. Cohn for helpful discussions, to the MIT Laser Research Center for the use of the Hamamatsu R2083 detector, to Tektronix for the loan of their 7250 transient digitizer, and to all those who helped take data.

This work was sponsored by the Department of the Navy for SDIO.

References

1. H. H. Barrett, "The Radon Transform and its Applications," in *Progress in Optics*, E. Wolf, Ed. (North-Holland, New York, 1984), p. 275.
2. Y. Das and W. M. Boerner, "On Radar Target Shape Estimation Using Algorithms for Reconstruction from Projections," IEEE Trans. Antennas Propag. **AP-26,** 274 (1978).
3. C. G. Bachman, *Laser Radar Systems and Techniques* (Artech House, Dedham, MA, 1979).
4. A. W. Rihaczek, *Principles of High-Resolution Radar* (McGraw-Hill, New York, 1969).
5. The required coherence time is related to the cross-range Doppler resolution d and the target rotation rate ω by $\tau = \lambda/(2\omega d)$. In cases of slowly rotating objects, the laser transmitter coherence time requirements may limit the achievable cross-range resolution and in some circumstances makes Doppler imaging impractical. In these cases, since the range resolution is independent of the target spin rate, range-resolved measurements are often still possible.
6. R. A. Brooks and G. Di Chiro, "Principles of Computer Assisted Tomography in Radiographic and Radioisotopic Imaging," Phys. Med. Biol. **21,** 689 (1976).
7. G. T. Herman, *Image Reconstruction from Projections* (Academic, New York, 1980).
8. N. H. Farhat, T. H. Chu, and C. L. Werner, "Tomographic and Projective Reconstruction of 3-D Image Detail in Inverse Scattering," in *Proceedings, SPIE Tenth International Optical Computing Conference* (Apr. 1983), pp. 82–88.

Influence of vertical stratification on the distribution of irradiance at the sea surface from a point source in the ocean

Howard R. Gordon

University of Miami, Physics Department, Coral Gables, Florida 33124.

Received 25 November 1987.
0003-6935/88/132643-03$02.00/0.

In this Letter, a bio-optical[1] model describing the distribution of irradiance at the sea surface resulting from a point source embedded in a homogeneous ocean is extended to a stratified ocean. In particular, the phytoplankton pigment concentration[2] C is allowed to vary with depth. Briefly, following Ref. 1, the absorption $a_C(z,\lambda)$ and scattering $b_C(z,\lambda)$ coefficients of the phytoplankton and their immediate detrital material at a wavelength λ are given by

$$b_C(z,\lambda) = B_C(\lambda)C(z)^{0.62},$$
$$a_C(z,\lambda) = 0.06A_C(\lambda)C(z)^{0.602}, \quad (1)$$